

HOKKAIDO UNIVERSITY

Title	Evidence for a secondary bow in Newton's zero-order nuclear rainbow
Author(s)	Ohkubo, S.; Hirabayashi, Y.
Citation	Physical Review C, 89(5), 051601 https://doi.org/10.1103/PhysRevC.89.051601
Issue Date	2014-05-08
Doc URL	https://hdl.handle.net/2115/56863
Rights	©2014 American Physical Society
Type	journal article
File Information	PhysRevC.89.051601.pdf



Hokkaido University Collection of Scholarly and Academic Papers : HUSCAP

PHYSICAL REVIEW C **89**, 051601(R) (2014)

Evidence for a secondary bow in Newton's zero-order nuclear rainbow

S. Ohkubo[1,2] and Y. Hirabayashi[3]

[1]*Research Center for Nuclear Physics, Osaka University, Ibaraki, Osaka 567-0047, Japan*

[2]*Department of Applied Science, Kochi Women's University, 5-15 Eikokuji-cho, Kochi 780-8515, Japan*

[3]*Information Initiative Center, Hokkaido University, Sapporo 060-0811, Japan*

(Received 12 December 2013; revised manuscript received 17 April 2014; published 8 May 2014)

Rainbows are generally considered to be caused by *static* refraction and reflection. A primary and a secondary rainbow appear due to refraction and internal reflection in a raindrop as explained by Newton. The quantum nuclear rainbow, which is generated by refraction in the nucleus droplet, only has a "primary" rainbow. Here we show for the first time evidence for the existence of a secondary nuclear rainbow generated dynamically by coupling to an excited state without internal reflection. This has been demonstrated for experimental $^{16}O + ^{12}C$ scattering using the coupled channel method with an *extended* double folding potential derived from microscopic *realistic* wave functions for ^{12}C and ^{16}O.

DOI: 10.1103/PhysRevC.89.051601 PACS number(s): 24.10.Eq, 24.10.Ht, 25.55.Ci

Newton, who explained the mechanism of the rainbow by refraction and reflection [1–3], believed in the existence of the zero-order rainbow without internal reflection in a droplet. Newton's zero-order rainbow [4] was realized in quantum systems when Goldberg *et al.* [5] observed a nuclear rainbow in high-energy α-particle scattering. The quantum nuclear rainbow is generated by the nuclear potential, which acts as a Luneburg lens [6], where refraction is the only active mechanism and a "primary" rainbow can only exist because there are no higher-order terms like in Nussenzveig's expansion for the meteorological rainbow [7]. We report here evidence for the unexpected existence of a secondary bow in the nuclear rainbow.

The nuclear rainbow is very important in determining the interaction potential family up to the internal region without discrete ambiguity [5] and has been studied extensively [8,9]. The nuclear rainbow is also powerful for studies of nuclear cluster structure in the bound and unbound energy regions. In fact, the global nuclear potential, which describes nuclear rainbow scattering for typical $\alpha + ^{16}O$, $\alpha + ^{40}Ca$, and $^{16}O + ^{16}O$ systems, can reproduce scattering over a wide range of incident energies and cluster structures of ^{20}Ne, ^{44}Ti, and ^{32}S in the bound and unbound energy regions, respectively, in a unified way [10–12]. In contrast to the $^{16}O + ^{16}O$ system, the Airy structure of the nuclear rainbow for the asymmetric $^{16}O + ^{12}C$ system, for which refraction is very strong, is clearly observed in experimental angular distributions without being obscured by symmetrization. For this system, a global potential that reproduces the energy evolution of the Airy minimum in the angular distributions over a wide range of incident energies at $E_L = 62 \sim 1503$ MeV [13–17] also successfully explains the cluster structure and molecular resonances with the $^{16}O + ^{12}C$ configuration in ^{28}Si in a unified way [18]. However, the global potential was confronted with a serious difficulty when a new measurement of the angular distribution in $^{16}O + ^{12}C$ scattering at $E_L = 281$ MeV up to $\theta \approx 100^\circ$ showed that an Airy minimum of the nuclear rainbow appears at the much larger angle $\theta \approx 70^\circ$ [19] than expected in the global potential ($\theta \approx 45^\circ$). It has been impossible to model a first-order Airy minimum $A1$ at this large angle with the established global potential [19]. Thus, the reason why the global potential fails to reproduce the Airy minimum of the nuclear rainbow at $E_L = 281$ MeV has been a mystery and raised a serious question of the common belief that nuclear rainbow scattering can determine the potential uniquely.

The purpose of this paper is to present for the first time evidence for the existence of a secondary nuclear rainbow in the $^{16}O + ^{12}C$ scattering generated dynamically by a quantum effect without internal reflections of classical concept, which is completely different from the Newton's meteorological secondary rainbow. We show that the Airy minimum at around $\theta \approx 70^\circ$, $A1^{(S)}$, is not a first-order Airy minimum, $A1^{(P)}$, of the well-known ("primary") nuclear rainbow due to the nuclear potential but a first-order Airy minimum of a *secondary* bow of the nuclear rainbow. The difficulty of the global potential is solved by the discovery of the secondary nuclear rainbow.

We study rainbow scattering for $^{16}O + ^{12}C$ with an extended double folding (EDF) model that describes all the diagonal and off-diagonal coupling potentials derived from the microscopic *realistic* wave functions for ^{12}C and ^{16}O using a density-dependent nucleon-nucleon force. The diagonal and coupling potentials for the $^{16}O + ^{12}C$ system are calculated using the EDF model without introducing a normalization factor:

$$V_{ij,kl}(\mathbf{R}) = \int \rho_{ij}^{(^{16}O)}(\mathbf{r}_1)\, \rho_{kl}^{(^{12}C)}(\mathbf{r}_2) \times v_{NN}(E,\rho,\mathbf{r}_1 + \mathbf{R} - \mathbf{r}_2)\, d\mathbf{r}_1 d\mathbf{r}_2, \quad (1)$$

where $\rho_{ij}^{(^{16}O)}(\mathbf{r})$ is the diagonal ($i = j$) or transition ($i \neq j$) nucleon density of ^{16}O taken from the microscopic $\alpha + ^{12}C$ cluster model wave functions calculated in the orthogonality condition model (OCM) in Ref. [20], which uses a realistic size parameter both for the α particle and ^{12}C and is an extended version of Ref. [21], which reproduces almost all the energy levels well up to $E_x \approx 13$ MeV and the electric transition probabilities in ^{16}O. The wave functions have been successfully used for the systematic analysis of elastic and inelastic $\alpha + ^{16}O$ scattering over a wide range of incident energies and the α cluster structure study of ^{20}Ne [22]. $\rho_{kl}^{(^{12}C)}(\mathbf{r})$ represents the diagonal ($k = l$) or transition ($k \neq l$) nucleon

 ©2014 American Physical Society

density of ^{12}C, which is calculated using the microscopic three-α-cluster model in the resonating group method [23]. This model reproduces the α cluster, α condensate, and shell-like structures of ^{12}C well and the wave functions have been checked for many experimental data, including charge form factors and electric transition probabilities. For the effective interaction $v_{\rm NN}$ we use the DDM3Y-FR interaction [24], which takes into account the finite-range nucleon exchange effect. An imaginary potential with a Woods-Saxon volume-type form factor is introduced phenomenologically to take into account the effect of absorption due to other channels.

First we show that the puzzling nuclear rainbow for the $^{16}\mathrm{O} + ^{12}\mathrm{C}$ system at $E_L = 281$ MeV cannot be explained by the traditional view that a rainbow is generated by a strong attractive nuclear potential. In Fig. 1, the angular distributions of elastic $^{16}\mathrm{O} + ^{12}\mathrm{C}$ scattering calculated using the conventional single-channel double-folding (DF) potential without channel couplings (blue solid lines) and the refractive farside components (dashed lines) are compared with the experimental data (points) at $E_L = 200 \sim 260$ MeV [15], 281 MeV [19], 300 MeV [25], 330 MeV [26], and 608 MeV [27]. For the imaginary potential, the strength parameter around 20 MeV was found to fit the data while the radius parameter and the diffuseness parameter were fixed at around 5.6 and 0.65 fm, respectively. The potential parameters used and the values of the volume integral per nucleon pair of the DF potential, J_V, are given in Table I. We found that the DF potential works well without introducing a normalization factor, values of the volume integral per nucleon pair are consistent with those used in other DF optical model calculations [14,15,17,25] and the DF potential used belongs to the same global potential family found in the $E_L = 62 \sim 124$ MeV [14] and $E_L = 132 \sim 1503$ MeV regions [15,17]. We see that the angular distributions are dominated by the refractive farside scattering. In Fig. 1, the discrepancies are clear for the data at $E = 281$, 300, and especially 330 MeV. It is evident that the theoretical calculations using a conventional single-channel DF potential fail to reproduce the experimental data at $281 \sim 330$ MeV. This shows that behavior not explained by the global potential (visualized by green points) is a nuclear rainbow that is not understood by the traditional concept of rainbow scattering.

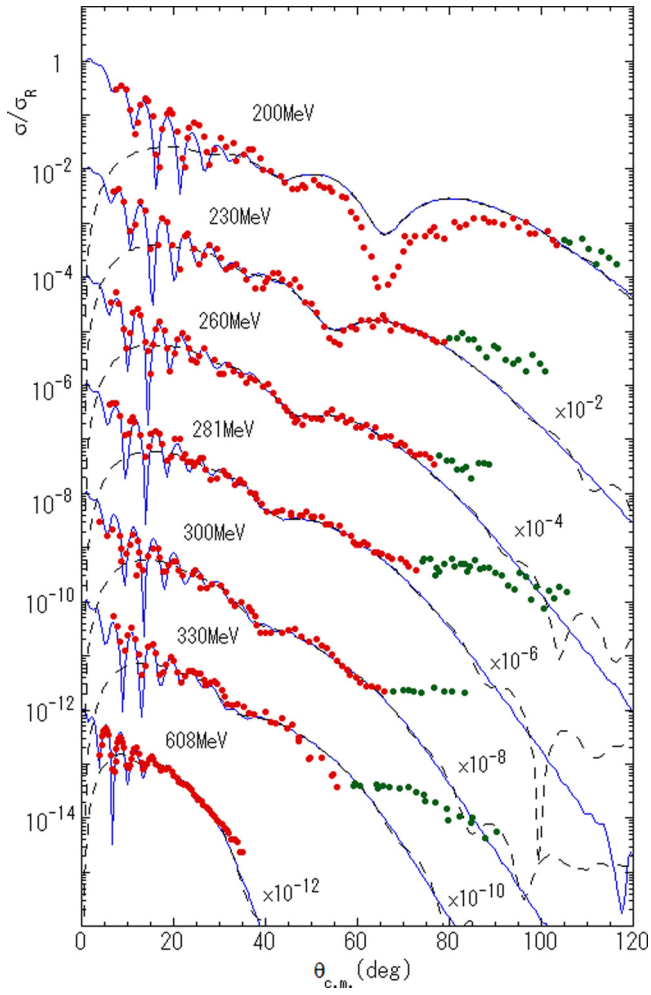


FIG. 1. (Color online) Comparison of the conventional single-channel DF potential calculations (blue solid line) with experimental angular distributions (red and green points) in $^{16}\mathrm{O} + ^{12}\mathrm{C}$ rainbow scattering [15,25–27]. The long dashed line displays the calculated farside components.

Next we show that the disagreement in Fig. 1 is not a drawback of the used global DF potential but a manifestation of the emergence of a new rainbow, which is beyond the optical potential model description of the nuclear rainbow in the Luneburg lens picture [6]. We calculate the $^{16}\mathrm{O} + ^{12}\mathrm{C}$ scattering with the EDF potential using CC method, which takes into account coupling to the excited 2^+ and 3^- states of the deformed ^{12}C at the excitation energy 4.44 and 9.64 MeV, respectively. The strength of the imaginary potential was slightly reduced since the channel coupling is explicitly introduced, and the radius parameter and the diffuseness parameter were fixed at around 5.6 and 0.75 fm, respectively (Table I). In Fig. 2, calculated angular distributions are displayed in comparison with the experimental data. We see that the agreement between the calculations (blue solid lines) and the experimental data is considerably improved compared with Fig. 1. (As discussed later, the larger oscillations than the data at the large angles are reduced by including additional coupling to the excited states of ^{16}O explicitly as displayed by the green thick solid line and the fit to the data is further improved.) The calculation reproduces the new Airy minimum of the nuclear rainbow in the experimental data at $281 \sim 330$ MeV well. The rainbow angle, θ_R, where the fall-off of the cross sections of the dark side of the rainbow scattering starts is shifted backward in accordance with the appearance of a new Airy minimum. Since the new minimum, $A1^{(S)}$, at around $\theta = 60 \sim 70^\circ$ just before the bump is caused by the farside scattering (dashed lines), it is clear that the new Airy minimum is produced by the refractive scattering with channel coupling. Even at $E_L = 200$, 230, and 260 MeV, the agreement of the calculated angular distribution with the experimental data is considerably improved in the regions $\theta > 100^\circ$, $\theta = 80^\circ \sim 100^\circ$, and $\theta = 70^\circ \sim 90^\circ$, respectively.

As shown at $E_L = 281$ and 330 MeV in Fig. 2, in creating a new Airy minimum, $A1^{(S)}$, at the larger angles the coupling to the 2^+ state is dominant, while the effect of the 3^- state is negligible and can be simply incorporated into the imaginary

TABLE I. The volume integral per nucleon pair J_V of the the ground-state diagonal potential and the imaginary potential parameters used in the single-channel double-folding calculations in Fig. 1 and coupled channels calculations with EDF in Fig. 2.

E_L	J_V	W_V	R_V	a_V	W_V	R_V	a_V	W_V	R_V	a_V
					(Coupled channels calculation with EDF)					
		(DF optical model)			(^{12}C excitation only)			(^{12}C and ^{16}O excitation)		
(MeV)	(MeV fm^3)	(MeV)	(fm)	(fm)	(MeV)	(fm)	(fm)	(MeV)	(fm)	(fm)
200	301	20.0	5.5	0.85	17.0	5.7	0.75	18.0	5.6	0.65
230	296	22.5	5.6	0.70	19.5	5.6	0.75	18.5	5.6	0.60
260	290	23.0	5.6	0.65	19.0	5.6	0.75	18.5	5.6	0.60
281	285	23.5	5.6	0.65	19.0	5.6	0.75	18.0	5.6	0.60
300	281	25.0	5.6	0.65	20.5	5.6	0.75	19.5	5.6	0.60
330	275	23.5	5.6	0.65	19.0	5.6	0.75	17.0	5.6	0.60
608	229	20.0	5.7	0.60	17.0	5.8	0.60	16.0	5.6	0.60

potential. Refraction via coupling to the 2^+ state plays the role of a dynamical secondary lens, which is completely different from the ordinary static lens of the nuclear potential interpreted as a Luneburg lens [6]. The effect of the dynamical lens is not possible to incorporate into the DF optical model potential as a normalization constant which is often used in the conventional DF model approach [28]. For this reason the global conventional DF optical model potential failed to reproduce the Airy structure in the 281 $\sim$ 330 MeV data in Fig. 1.

By investigating the deflection function we show that this new Airy minimum, $A1^{(S)}$, of the nuclear rainbow in the range 281 $\sim$ 330 MeV is due to a *secondary nuclear rainbow*, which is dynamically generated in the classically forbidden angular region, i.e., in the dark side of the ordinary "primary" nuclear rainbow. In Fig. 3 the deflection functions determined from the phase shifts calculated in the CC method and in the conventional DF optical model without imaginary potential are displayed at 330 MeV. In the conventional DF optical model calculation we see a single minimum at the orbital angular momentum $L_R = 27$ with the rainbow angle $\theta_R = 63^\circ$ consistent with the textbook fact that the nuclear rainbow is caused by a refraction in the nuclear attractive potential [29]. On the other hand, in the CC calculation the deflection function is drastically changed to have more than two extrema, which means the existence of more than two nuclear rainbows in elastic scattering by a new mechanism. The investigation of the S matrix shows that the coupling to the 2^+ state is very strong for the relevant $L = 20 \sim 35$ region, especially at the minima. The two extrema at $L_{R0} = 31$ with $\theta_{R0} = 18^\circ$ and at $L_{R1} = 34$ with the rainbow angle $\theta_{R1} = 43^\circ$ are located at forward angles, while the minimum with the largest rainbow angle $\theta_{R2} = 95^\circ$ appears at $L_{R2} = 26$. In contrast to the meteorological rainbow, the bright sides of the two rainbows where the Airy maximum and minimum appear with θ_{R1} ("primary" nuclear rainbow) and θ_{R2} (secondary nuclear rainbow) stand on the same side of the nuclear rainbow. Therefore, the dark side of the "primary" nuclear rainbow where the cross sections fall toward large angles in the angular distribution is masked by the bright side of the secondary nuclear rainbow and difficult to observe. The experimental Airy minimum at the large angles, $A1^{(S)}$, and the fall-off are due to this secondary nuclear rainbow and it is reasonable that the conventional global DF optical model with a single deflection minimum, which creates an Airy minimum, $A1^{(P)}$, of the "primary" nuclear rainbow due to the nuclear potential, cannot reproduce the Airy minimum of the secondary nuclear rainbow at 281 $\sim$ 300 MeV. The precursor of the secondary nuclear rainbow can already be seen in the poor agreement of the calculated angular distributions in the conventional DF optical model at 260 MeV in Fig. 1. It is startling that a secondary nuclear rainbow appears for the nuclear system where the active mechanism is only refractive. This has not been anticipated from the meteorological secondary rainbow for which reflection is involved [1–3,7,29]. A dynamical second lens is only possible in a quantum system such as the ^{16}O + ^{12}C scattering as demonstrated in this paper. The traditional view that the rainbow is generated by *static* refraction and reflection of classical concept is changed in nuclear context.

In Fig. 4 calculated results without and with the imaginary potentials are compared. We can confirm that the Airy minimum $A1^{(S)}$, which appears also in the absence of the imaginary potential, is entirely due to the real potential and is created by coupling to the 2^+ state of ^{12}C.

We investigate the effects of the channels coupling to the excited states of ^{16}O on the creation of the Airy minimum $A1^{(S)}$. In Fig. 2 the angular distributions calculated including the channels coupling of the ground state to the excited states, 3^- (6.13 MeV) and 2^+ (6.92 MeV), of ^{16}O in addition to the excited states of ^{12}C are displayed by the green thick solid line. Potential parameters used are given in Table I. We see that the large oscillations at large angles seen in the blue lines are suppressed and the agreement with the experimental data is improved further especially at the large angles around and beyond the Airy minimum. This coupling tends to obscure the deep Airy minimum created by coupling to the 2^+ state of ^{12}C as an imaginary potential generally does. These results show that the Airy minimum $A1^{(S)}$ is due to the 2^+ state of ^{12}C. Our CC calculations using the imaginary potentials interpolated from E_L =330 and 608 MeV predict the persistency of the Airy minimum of the nuclear rainbow at the higher energies between $E_L = 350$ and 500 MeV. Especially at around

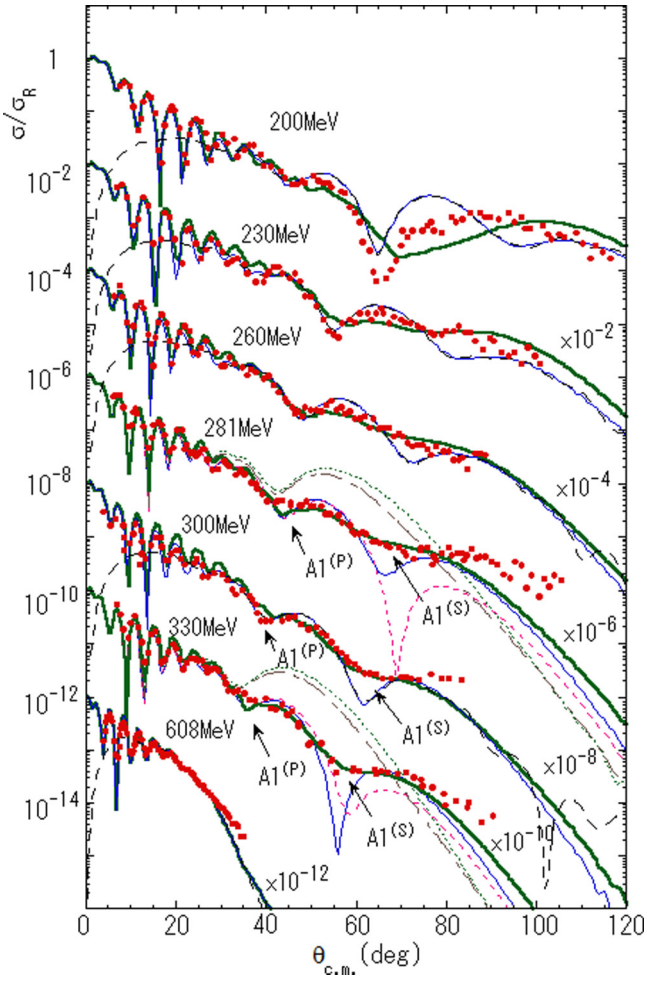


FIG. 2. (Color online) Same as described in the legend of Fig. 1 except for the CC calculations. The calculated cross sections with coupling to the 2^+ and 3^- states of ^{12}C (blue solid line) and the farside components (long dashed line) are displayed in comparison with the experimental data (points) [15,25–27]. The calculations with coupling to the 2^+ state only (pink dashed line), 3^- state only (dashed dotted line), and no coupling (dotted line) are shown for $E_L = 281$ and 330 MeV. The Airy minimum of the "primary" nuclear rainbow, $A1^{(P)}$, and that of the secondary nuclear rainbow, $A1^{(S)}$, are indicated. The CC calculations including coupling of the ground state to the 3^- and 2^+ states of ^{16}O in addition to coupling to the 2^+ and 3^- states of ^{12}C are displayed by the green thick solid line (see text).

$E_L = 400$ MeV a clear deep Airy minimum, which is hardly obscured by the coupling to the excited states of ^{16}O, is predicted. The experimental observation of the Airy minimum at these energies is expected.

Finally, we will make a brief discussion on the contribution of the transfer reaction channels. As for the elastic transfer of α particles [30], we see in the recent coupled reaction channel calculations of Ref. [31] that the exchange of the α particle (elastic transfer) is three orders of magnitude smaller than the elastic scattering cross sections. Although a complete description of the data may require both inelastic and exchange couplings, as for the one nucleon exchange effect, which is suggested to prevail over other transfer reactions to affect

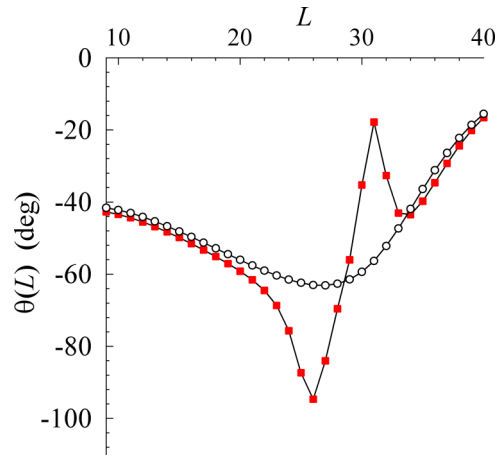


FIG. 3. (Color online) The deflection functions calculated from the real DF optical model (circle) and the CC method (square) with the EDF potential at $E_L = 330$ MeV are compared. The line is to guide the eye.

the Airy minimum $A1^{(S)}$ for the 230 MeV data in Ref. [31], our calculations take into account it by using the effective interaction DDM3Y, in which the knock-on exchange effect is incorporated [24,28].

To summarize, we have shown for the first time the evidence for the existence of a secondary bow in the Newton's zero-order nuclear rainbow by analyzing $^{16}\mathrm{O} + ^{12}\mathrm{C}$ scattering using a coupled channel method with an extended double folding (EDF) potential derived from the microscopic *realistic* wave functions for ^{12}C and ^{16}O. The secondary nuclear rainbow appears dynamically in the classically forbidden angular region of the dark side of the ordinary "primary" nuclear rainbow due to the creation of a new rainbow angle caused by strong coupling to the 2^+ state of ^{12}C. This plays the

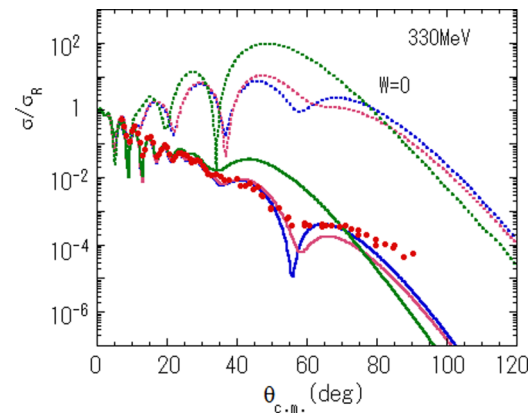


FIG. 4. (Color online) Angular distributions in $^{16}\mathrm{O} + ^{12}\mathrm{C}$ scattering at $E_L = 330$ MeV calculated in the single channel (green solid line) and CC method (blue and pink solid line) with the imaginary potential in Table I are compared with those calculated by switching off the imaginary potential (dotted line) and the experimental data (points) [26]. The blue and pink lines represent the CC results with coupling to the 2^+ and 3^- states of ^{12}C and those with coupling to the 2^+ state of ^{12}C only, respectively.

role of a second lens in addition to the static lens caused by the nuclear potential. The traditional view that the rainbow is understood by the classical concept of refraction and reflection is changed in nuclear context. The discovery of a secondary rainbow solves the dilemma concerning the failure of the global potential for the $^{16}O + ^{12}C$ system. It is desired to observe a secondary rainbow in other systems.

One of the authors (S.O.) thanks the Yukawa Institute for Theoretical Physics for the hospitality extended during a stay in February 2013. Part of this work was supported by the Grant-in-Aid for the Global COE Program "The Next Generation of Physics, Spun from Universality and Emergence" from the Ministry of Education, Culture, Sports, Science, and Technology (MEXT) of Japan.

[1] I. Newton, *Opticks or a Treatise of the Reflexions, Refractions, Inflexions, and Colours of Light* (Dover publications, New York, 1952).
[2] H. M. Nussenzveig, Sci. Am. **236**, 116 (1977).
[3] J. A. Adam, Phys. Rep. **356**, 229 (2002).
[4] C. F. Bohren and A. B. Fraser, Am. J. Phys. **59**, 325 (1991).
[5] D. A. Goldberg and S. M. Smith, Phys. Rev. Lett. **29**, 500 (1972); D. A. Goldberg, S. M. Smith, and G. F. Burdzik, Phys. Rev. C **10**, 1362 (1974).
[6] F. Michel, G. Reidemeister, and S. Ohkubo, Phys. Rev. Lett. **89**, 152701 (2002).
[7] H. M. Nussenzveig, J. Math. Phys. **10**, 82 (1969); **10**, 125 (1969).
[8] D. T. Khoa, W. von Oertzen, H. G. Bohlen, and S. Ohkubo, J. Phys. G **34**, R111 (2007).
[9] R. Anni, Phys. Rev. C **63**, 031601(R) (2001).
[10] F. Michel, S. Ohkubo, and G. Reidemeister, Prog. Theor. Phys. Suppl. **132**, 7 (1998).
[11] S. Ohkubo, T. Yamaya, and P. E. Hodgson, in *Nucleon-Hadron Many-Body Systems*, edited by H. Ejiri and H. Toki (Oxford University Press, Oxford, 1999), p. 150.
[12] S. Ohkubo and K. Yamashita, Phys. Rev. C **66**, 021301(R) (2002).
[13] A. A. Ogloblin *et al.*, Phys. Rev. C **57**, 1797 (1998).
[14] M. P. Nicoli *et al.*, Phys. Rev. C **61**, 034609 (2000).
[15] A. A. Ogloblin *et al.*, Phys. Rev. C **62**, 044601 (2000).
[16] S. Szilner *et al.*, Phys. Rev. C **64**, 064614 (2001).
[17] D. T. Khoa, W. von Oertzen, and H. G. Bohlen, Phys. Rev. C **49**, 1652 (1994).
[18] S. Ohkubo and K. Yamashita, Phys. Lett. B **578**, 304 (2004).
[19] A. A. Ogloblin *et al.*, Phys. At. Nucl. **66**, 1478 (2003).
[20] S. Okabe, *Tours Symposium on Nuclear Physics II*, edited by H. Utsunomiya *et al.* (World Scientific, Singapore, 1995), p. 112.
[21] Y. Suzuki, Prog. Theor. Phys. **55**, 1751 (1976); **56**, 111 (1976).
[22] Y. Hirabayashi and S. Ohkubo, Phys. Rev. C **88**, 014314 (2013).
[23] M. Kamimura, Nucl. Phys. A **351**, 456 (1981).
[24] A. M. Kobos *et al.*, Nucl. Phys. A **384**, 65 (1982); **425**, 205 (1984).
[25] M. E. Brandan *et al.*, Nucl. Phys. A **688**, 659 (2001).
[26] A. S. Dem'yanova *et al.*, IAEA Database exfor, http://www-nds.iaea.org/exfor/.
[27] M. E. Brandan *et al.*, Phys. Rev. C **34**, 1484 (1986).
[28] M. E. Brandan and G. R. Satchler, Phys. Rep. **285**, 143 (1997).
[29] R. G. Newton, *Scattering Theory of Waves and Particles* (McGraw-Hill Book Company, New York, 1966).
[30] S. Szilner *et al.*, Eur. Phys. J. A **13**, 273 (2002).
[31] A. T. Rudchik *et al.*, Eur. Phys. J. A **44**, 221 (2010).